Nucleic Acids Research, 2019 **1**
doi: 10.1093/nar/gkz202

Modulation of HIV-1 Gag/Gag-Pol frameshifting by tRNA abundance

Natalia Korniy[1], Akanksha Goyal[1], Markus Hoffmann[2], Ekaterina Samatova[1], Frank Peske[1], Stefan Pöhlmann[2,3] and Marina V. Rodnina[1,*]

[1]Department of Physical Biochemistry, Max Planck Institute for Biophysical Chemistry, Am Fassberg 11, 37077 Göttingen, Germany, [2]Infection Biology Unit, German Primate Center, Kellnerweg 4, 37077 Göttingen, Germany and [3]Faculty of Biology and Psychology, University of Göttingen, Wilhelm-Weber-Str. 2, 37073 Göttingen, Germany

Received February 11, 2019; Revised March 12, 2019; Editorial Decision March 14, 2019; Accepted April 08, 2019

ABSTRACT

A hallmark of translation in human immunodeficiency virus type 1 (HIV-1) is a –1 programmed ribosome frameshifting event that produces the Gag-Pol fusion polyprotein. The constant Gag to Gag-Pol ratio is essential for the virion structure and infectivity. Here we show that the frameshifting efficiency is modulated by Leu-tRNA^{Leu} that reads the UUA codon at the mRNA slippery site. This tRNA^{Leu} isoacceptor is particularly rare in human cell lines derived from T-lymphocytes, the cells that are targeted by HIV-1. When UUA decoding is delayed, the frameshifting follows an alternative route, which maintains the Gag to Gag-Pol ratio constant. A second potential slippery site downstream of the first one is normally inefficient but can also support –1-frameshifting when altered by a compensatory resistance mutation in response to current antiviral drug therapy. Together these different regimes allow the virus to maintain a constant –1-frameshifting efficiency to ensure successful virus propagation.

INTRODUCTION

Many viruses use programmed ribosome frameshifting to increase the coding capacity of their genome and to regulate stoichiometric ratio between viral proteins (1–4). The two HIV-1 genes, *gag* and *pol*, encode viral structural proteins and enzymes, respectively, and overlap by 205 nt. Synthesis of the Gag-Pol polyprotein requires –1 ribosome frameshifting (–1FS) (5). The ratio between Gag and Gag-Pol is crucial for virus propagation and its dysregulation is detrimental for replication, virion formation and infectivity of HIV-1 (6–9). The efficiency of gag-pol –1FS in human cells is about 10%, ranging from 2% to 11% with different reporters (10–13). This –1FS efficiency has been recapitulated *in vivo* or *in vitro* in mammalian, yeast or *Escherichia coli* translation extracts (5,11,14–22), suggesting that the virus exploits evolutionary conserved features of the translational apparatus.

–1FS is governed by two cis-acting elements in the mRNA, the slippery site (SS1) U_1 UUU_4 UUA_7 that encodes Phe (UUU) and Leu (UUA) in the 0-frame (5), and a stem-loop (SL) structure downstream of the slippery site (SL1; Figure 1A). SS1 gives rise to two frameshifting products, one that contains the 0-frame peptide Phe-Leu followed by the –1-frame sequence (FLR product; Figure 1A and B), and another with a second Phe incorporated instead of Leu (FFR product). In mammalian cells ∼30% of frameshifting ribosomes do not insert Leu, but are likely to insert Phe at the same position (5). Also in *E. coli*, both products are produced, with the FLR constituting about 80% of the product (5,15,23,24). Further HIV frameshifting product heterogeneity may result from –2 frameshifting (25). In addition, the *gag-pol* gene has a second, putative slippery site (pSS2) 38 nt downstream of the canonical SS1 (26–30). This slippery site is also conserved albeit to a lesser degree than the first slippery site (31). The sequence of pSS2 (U_1 UUU_4 CUU_7) is not particularly slippery, but a substitution of C_5 with U (C_5U), which appears as a compensatory resistance mutation during anti-HIV therapy, may facilitate additional FS at this otherwise silent site (26–28,30).

The mechanism of frameshifting on the gag-pol mRNA and the factors that define the ratio between the two –1FS products are unclear. The variety of proposed mechanisms of –1FS (23), the uncertain significance of the second slippery site, and the lack of mechanistic information about alternative slippages (e.g., –2FS or +1FS) have prompted us to study gag-pol frameshifting in real time in a fully reconstituted *in vitro* translation system. We show that FS pathway and efficiency are determined by the availability of Leu-tRNA^{Leu} reading the UUA codon. The potential alternative +1 and –2 slippages can also operate when other aminoacyl-tRNAs (aa-tRNAs) are in limited supply. We show that the UUA-specific tRNA^{Leu} is particularly rare in human cell

*To whom correspondence should be addressed. Tel: +49 551 201 2900; Fax: +49 551 201 2905; Email: rodnina@mpibpc.mpg.de

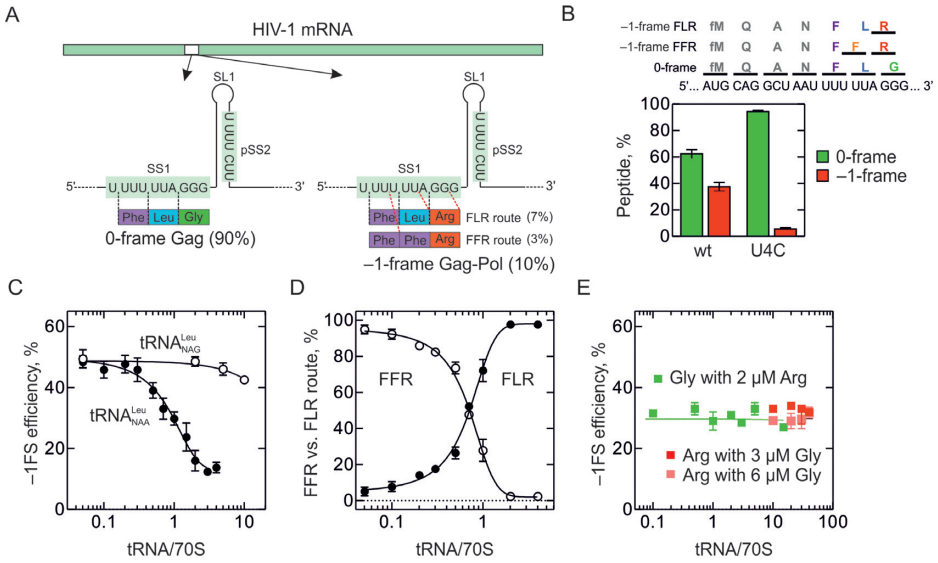

Figure 1. –1FS on HIV-1 gag-pol mRNA. (**A**) Scheme of the gag-pol frameshifting site. Slippery site (SS1) and the putative second slippery site (pSS2) are highlighted in green; the stimulatory mRNA structure element downstream of the SS1 is indicated as a stem-loop (SL1). Amino acids incorporated into 0-frame and –1-frame peptides as well as the potential –1FS routes and *in vivo* efficiencies are shown below the frameshifting sites. (**B**) Top panel: Amino acids incorporated into 0- and –1-frames are shown above the mRNA sequence. Bottom panel: –1FS efficiency with the wild-type (wt) mRNA and U_4C derivative with disrupted SS1 measured at limiting amounts of Leu-$tRNA_{NAA}^{Leu}$ (molar ratio 0.3 tRNA to 70S ribosome) at the end of translation (2 min). The 0-frame is the sum of MQANF and MQANFLG peptides, –1-frame corresponds to MQANFFR/FLR peptides. MQANF was identified based on its position on the chromatogram while MQANFFR/FLR and MQANFLG products were quantified using [^{14}C]Arg and [^{3}H]Gly, respectively. (**C**) Concentration dependence of –1FS efficiency on the Leu-$tRNA_{NAA}^{Leu}$ ($tRNA_{NAA}^{Leu}$, closed circles) or a mixture of $tRNA^{Leu}$ isoacceptors reading CUN codons ($tRNA_{NAG}^{Leu}$, open circles). –1FS product was detected using [^{14}C]Arg. (**D**) Change in the FS regime with the Leu-$tRNA_{NAA}^{Leu}$ concentration. The ratio of FFR route (open circles) versus FLR (closed circles) route was calculated from peptides with different radioactive labels as follows. The sum of FFR and FLR frameshifting products was calculated using [^{14}C]Arg. To determine the amount of FLR, the mRNA was translated to the 0-frame peptide fMet-Gln-Asn-Phe-Leu-Gly-Lys-Ile (MQANFLGKI). The presence of Ile allows for separation between 0-frame MQANFLGKI and –1-frame MQANFLR peptides. The FFR peptide was then determined by subtracting the FLR from the total Arg-containing product. (**E**) –1FS efficiency in the presence of varying concentrations of Gly-$tRNA^{Gly}$ in the presence of excess Arg-$tRNA^{Arg}$ (2 μM) (green squares) or with varying concentrations of Arg-$tRNA^{Arg}$ in the presence of 3 or 6 μM Gly-$tRNA^{Gly}$ (red and light red squares, respectively).

lines derived from T-lymphocytes, the cells that are targeted by HIV-1. Furthermore, we have characterized the role of the second slippery site in supporting –1FS. Multiple ways to modulate the frameshifting efficiency could help the virus to maintain the Gag to Gag-Pol ratio, which is crucial for its viability.

MATERIALS AND METHODS

Buffer

All experiments with prokaryotic translation components, including kinetic measurements summarized in Supplementary Table S1, were carried out in HiFi buffer (50 mM Tris–HCl, pH 7.5, 70 mM NH_4Cl, 30 mM KCl, 3.5 mM $MgCl_2$, 8 mM putrescine, 0.5 mM spermidine, 1 mM 1,4-dithiothreitol (DTT)) at 37°C if not stated otherwise.

tRNA preparation

70S ribosomes from *E. coli* MRE600, initiation factors (IF1, IF2, IF3), elongation factors (EF-Tu, EF-G), RF1, fMet-$tRNA^{fMet}$, BODIPY-Met-$tRNA^{fMet}$ and Phe-$tRNA^{Phe}$ were prepared from *E. coli* as described (32,33–39). Gln-, Ala- and Asn-tRNA mixture, Arg-$tRNA^{Arg}$, Gly-$tRNA^{Gly}$, Val-$tRNA^{Val}$ were prepared from *E. coli* total tRNA by aminoacylation with the respective amino acid and subsequent affinity chromatography of the EF-Tu–GTP–aa-tRNA ternary complexes on Protino Ni-IDA 2000 Packed Columns (Macherey-Nagel) followed by phenolization and ethanol precipitation of aa-tRNA. $tRNA_{NAA}^{Leu}$, elongator $tRNA^{Met}$, $tRNA^{Tyr}$ and a mixture of isoacceptors $tRNA^{Leu}$ collectively reading all four CUN codons for Leu were prepared by consecutive column chromatographies on Sepharose 4B (GE Healthcare), Phenyl Sepharose (GE Healthcare), and DEAE Toyopearl (Tosoh Bioscience). $tRNA^{Trp}$ was prepared by T7 RNA-polymerase transcription from pUC18 plasmid carrying the *E. coli trp* gene (40). tRNAs were charged with ^{14}C-, or ^{3}H-labeled or unlabeled amino acids (41). Leu-$tRNA_{NAA}^{Leu}$, mixture of isoacceptors Leu-tRNA for the CUN codons, Met-$tRNA_e^{Met}$, Ile-$tRNA^{Ile}$ and Tyr-$tRNA^{Tyr}$ were purified by reversed-phase HPLC on a WP-300 RP-18 column (250 mm × 10.5 mm, Merck) equilibrated with 20 mM ammonium acetate, pH 5.0, 10 mM magnesium acetate, 400 mM NaCl using a gradient of 0 to 15% ethanol. Concentrations were determined spectrophotometrically at 260 nm and by liquid–liquid scintillation counting where applicable (Ultima Gold XR, Perkin Elmer). Total human aa-tRNA was prepared from HeLa S10 cell extracts. The cytoplasmic fraction of the cell lysate was phenolized and aa-tRNA was purified by anion-exchange chromatography on a HiTrap Q HP column (5 ml, GE Healthcare) equilibrated with 50 mM

sodium acetate, pH 4.5 and 10 mM $MgCl_2$ using a gradient of 0 to 1.1 M KCl.

mRNA constructs

We used a native sequence of the gag-pol HIV-1 frameshifting motif (nt 1601–1961 in the HIV-1 complete genome, NCBI Reference Sequence NC_001802.1) cloned into pEX-A2 vector. Mutations were introduced by site-directed mutagenesis using Q5 DNA-polymerase (NEB) (42) (Supplementary Tables S2–S4). mRNAs were prepared by *in vitro* transcription with T7 RNA-polymerase (43,44) and purified using the RNeasy maxi kit (Qiagen) according to the manufacturer's recommendations. Control mRNAs used to determine the rate of Arg-$tRNA^{Arg}$ incorporation in 0-frame (Supplementary Figure S3B) were made by chemical synthesis (IBA, Göttingen) and contained an *E. coli* Shine-Dalgarno (SD) sequence inserted 9 nt upstream of the start codon AUG. For translation in bacterial translation system, a SD sequence was inserted into the HIV mRNA 6 nt upstream of the start codon AUG. In the short mRNAs used in the codon walk experiments, AUG was introduced 8 nt upstream of the SS1 and the length of the sequence following the SS1 was 56 nt encompassing SL1 and pSS2. In the mRNAs used to study +1 and –2 frameshifting, the GGG codon (Gly) following the slippery site was mutated to UGG (Trp) to distinguish between the –1-, –2- and +1-frameshifting products (10). The nearest natural AUG in gag mRNA was used as a start codon in the long mRNAs to study gag-pol translation products by PAGE. The stop codon UAG was introduced in the 0-frame 156 nt downstream of the AUG and 120 nt after the SS1 to allow the separation between the 0-frame (52 aa) and –1-frame (120 aa) products. 0-, –1- and –2-frame control mRNAs contain respective sequence cloned in-frame with SS1 and pSS2 being mutated to prevent slippages; these mRNAs contained 324 nt after the SS1 harboring SL1, pSS2 and pSL2. HIV mRNAs for eukaryotic translation contained the native 5' UTR from rabbit β-globin mRNA and a Kozak sequence with an embedded AUGG site to allow for efficient initiation. The start codon AUG was placed 8 nt upstream of the slippery site, and the next codon CAG (Gln) was mutated to GAG (Val) to improve initiation and facilitate product separation by HPLC. Eukaryotic mRNAs contained 167 nt downstream of SS1 covering SL1, pSS2 and pSL2. All mRNA sequences are listed in Supplementary Tables S2–S4 (AUG is in bold, slippery sites are underlined, UAG stop codon in 0-frame is in italic and mutated nucleotides are in small letters in bold).

Preparation of initiation complexes

70S initiation complexes (IC) were prepared by incubating 70S ribosomes (1 μM) with mRNA (3–10 μM), initiation factors IF1, IF2 and IF3 (1.5 μM each), initiator f[^{3}H]Met-$tRNA^{fMet}$ or BODIPY-Met-$tRNA^{fMet}$ (2 μM), DTT (1 mM) and GTP (1 mM) in HiFi buffer for 30 min at 37°C. ICs used in the codon-walk experiments were purified by ultracentrifugation through a 1.1 M sucrose cushion in buffer A (50 mM Tris-HCl pH 7.5, 70 mM NH_4Cl, 30 mM KCl, 7 mM $MgCl_2$) and dissolved in HiFi buffer.

Codon-walk assay

To form EF-Tu–GTP–aa-tRNA ternary complexes (TCs), EF-Tu (25–30 μM or 3-fold excess over aa-tRNA) was incubated with GTP (1 mM), phosphoenolpyruvate (3 mM) and pyruvate kinase (0.1 mg/ml) in buffer A with DTT (1 mM) for 15 min at 37°C. Then aa-tRNAs were added and incubated for 1 min at 37°C. The concentrations of aa-tRNAs were optimized to ensure the maximum binding at their respective codon: 1.6 μM each for Gln-$tRNA^{Gln}$, Ala-$tRNA^{Ala}$, Asn-$tRNA^{Asn}$, Phe-$tRNA^{Phe}$ and Arg-$tRNA^{Arg}$, 1.2 μM for Gly-$tRNA^{Gly}$, and different concentrations of Leu-$tRNA_{NAA}{}^{Leu}$ as indicated. IC (0.16 μM) was mixed with TCs (about 20 μM final concentration of EF-Tu), EF-G (1.6 μM), GTP (1 mM) phosphoenolpyruvate (2.4 mM) and pyruvate kinase (0.08 mg/ml) in HiFi buffer at 37°C. Incubation times were 0–10 min for time courses or 2 min for end-point measurements. The stability of peptidyl-tRNA binding to the ribosome was tested by nitrocellulose filter binding assay (Supplementary Figure S3D). To prepare samples for the HPLC analysis, the reactions were quenched with KOH (0.5 M) and hydrolyzed for 30 min at 37°C; then the samples were neutralized by the addition of acetic acid. Translation products were separated by reversed-phase HPLC on an RP-8 column (LiChroSpher100, Merck) applying an adapted gradient of acetonitrile (0–65%) with 0.1% trifluoroacetic acid. Eluted fractions were mixed with Ultima Gold XR scintillation liquid (Perkin Elmer) and analyzed by scintillation counting. The peptide products up to MQAN were not separated from each other, while all other peptides could be identified by either position shift on a chromatogram or by the radioactive label of the respective amino acid. The amount of each product was determined as a ratio between ^{3}H-counts in the respective peak and total ^{3}H-counts in the eluate. For samples with [^{3}H]Gly-$tRNA^{Gly}$, [^{14}C]Arg-$tRNA^{Arg}$ or [^{14}C]Leu $tRNA_{NAA}{}^{Leu}$, the respective peaks were calculated in pmol. Where necessary, the amount of MQANFLR peptide was calculated by subtracting MQANFLG from MQANFL in pmol. Likewise, the MQANFFR peptide was calculated by subtracting MQANFLR from the MQANFLR/FFR mixture product in pmol. Time courses were evaluated by numerical integration in KinTek Explorer software (45). Frameshifting efficiency was calculated as a ratio between the –1-frame peptide (MQANFFR and MQANFLR) and the sum of –1- and all 0-frame peptides (MQANF, MQANFL, MQANFLG) multiplied by 100%.

End-point translation assay of –2 / +1 mRNA

Translation of –2 / +1 mRNA was carried out as described for the codon-walk assay, but with 0.4 μM of each Gln-$tRNA^{Gln}$, Ala-$tRNA^{Ala}$, Asn-$tRNA^{Asn}$, 0.8 μM of Phe-$tRNA^{Phe}$, 0.08 μM of Leu-$tRNA_{NAA}{}^{Leu}$ and 0.4 μM each of Trp-$tRNA^{Trp}$, Met-$tRNA_e{}^{Met}$ and Tyr-$tRNA^{Tyr}$. IC (0.08 μM) was mixed with TCs (about 10 μM final concentration of EF-Tu), EF-G (1.6 μM), GTP (1 mM) phosphoenolpyruvate (2.4 mM) and pyruvate kinase (0.08 mg/ml) in HiFi buffer at 37°C. The efficiency of frameshifting peptide synthesis was calculated by dividing the amount of the re-

spective peptide in pmol by the sum of all peptides in translation excluding MQAN multiplied by 100%.

Arg-tRNA^{Arg} incorporation assay

To form post-translocation complexes, purified ICs (0.16 μM final) were mixed with Phe-tRNA^{Phe} (1.6 μM) or Leu-tRNA$_{NAA}^{Leu}$ (0.16 μM) in the presence of EF-G (0.008 μM, 1/20 of the IC concentration) in HiFi buffer and incubated for 1 min at 37°C. Post-translocation complexes were then mixed with Arg-tRNA^{Arg} (1.6 μM) and EF-G (1.6 μM) and reacted for 1 to 100 s at 37°C. The position of MFR and MLR peptides was identified based on [^{14}C]Arg counts and their amounts were calculated in pmol. The rate of Arg incorporation was estimated by exponential fitting in GraphPad Prism software.

Translation assay

IC prepared with BODIPY-Met-tRNA^{fMet} (0.08 μM) was incubated with EF-Tu (80 μM), total aa-tRNA from HeLa cells (3–10 μM), EF-G (1.6 μM) and RF1 (0.8 μM), GTP (1 mM), phosphoenolpyruvate (2.4 mM) and pyruvate kinase (0.08 mg/ml) in HiFi buffer at 37°C as indicated in the time course of translation or for 30 min for single-point measurements. In case of γB-crystallin, translation was carried out using IC (0.02 μM), EF-Tu (45 μM), total aa-tRNA from HeLa (10 μM), EF-G (1 μM), GTP (0.8 mM), phosphoenolpyruvate (1.4 mM) and pyruvate kinase (0.05 mg/ml) for 30 min in HiFi buffer at 37°C. To prepare the samples for PAGE, the reactions were stopped with NaOH (0.4 M) and hydrolyzed as described for the HPLC sample preparation. HEPES (0.2 M, pH 5) was added to neutralize the reactions. The samples were separated by Tris-Tricine gel electrophoresis (46). Fluorescent peptides were visualized using an Typhoon™ FLA-9000 scanner (GE Healthcare Life Sciences) and the band intensities were evaluated using the MultiGauge software. Frameshifting efficiency was calculated from the band intensities of the –1-frame product to the sum of –1- and 0-frames products as well as of translation intermediates appearing at 20 s of translation. The correct length of the peptides was confirmed using control 0-frame, –1-frame and –2-frame mRNAs.

Translation of HIV mRNAs in a fully reconstituted homologous mammalian *in vitro* translation system

40S and 60S ribosomal subunits from HeLa, translation initiation factors eIF1, eIF1A, eIF2, eIF3, eIF4A, eIF4B, eIF5, eIF5B, translation elongation factors eEF1A and eEF2 as well as Met-tRNA^{Met} were prepared according to published protocols (47,48).

48S IC (0.3 μM) was formed by incubating 40S subunits with a 2-fold molar excess of eIF2, eIF3 and eIF4B, a 3-fold excess of eIF1, eIF1A and eIF4A, a 3-fold excess of mRNA and a 5-fold excess of [^{3}H]Met-tRNA^{Met} in mammalian translation (MT) buffer (20 mM Tris–HCl, pH 7.5, 100 mM KCl, 2.5 mM $MgCl_2$, 0.25 mM spermidine, 1 mM ATP and 0.5 mM GTP) for 15 min at 37°C. To form 80S IC, an equal volume of MT buffer containing eIF5 (0.4 μM), eIF5B (0.5 μM) and 60S subunits (0.6 μM) was added. The initiation reaction mix was incubated for 8 min at 37°C.

An elongation reaction mix was prepared by incubating eEF1A (10.5 μM), eEF2 (5 μM), elongator tRNA mix (100 μM total human tRNA aminoacylated with Val, Ala, Asn, Phe, Leu, Arg, and Gly), phosphoenol pyruvate (3 mM), 1 mM $MgCl_2$ and pyruvate kinase (0.1 μg/μl) in MT buffer for 8 min at 37°C. In experiments shown in Supplementary Figure 4F [^{14}C]Leu and [^{3}H]Arg were used; in Figure 5F only [^{3}H]Arg was radioactive labeled. To start translation, an equal volume of the elongation reaction mix was added to the initiation reaction mix and incubated for 4 min at 37°C. Sample preparation for HPLC, HPLC analysis and quantification of radioactive peptides were done as described above for the bacterial translation system. –1-frame peptides were identified based on [^{3}H]Arg. In the presence of Leu, total translation efficiency was quantified using [^{14}C]Leu and the frameshifting efficiency was calculated as a ratio between Arg-containing peptides and total translation products multiplied by 100%. In the absence of Leu, total translation efficiency was calculated using –1-frame control, which shows the maximum level of frameshifting peptide produced under the given conditions. Here the frameshifting efficiency was calculated as the ratio between Arg-containing wt peptides and –1-frame control peptides multiplied by 100%.

Quantification of tRNA levels using qRT-PCR

Sup-T1 cells were derived from non-Hodgkin's T-cell lymphoma isolated from a pleural effusion of an 8-year-old male and subcloned on soft agar. Jurkat cells were derived from human T-cell lymphoblast. PM1 cells are a derivative of HUT78, a human cutaneous T-cell lymphoma cell line derived from peripheral blood of a patient with Sezary syndrome. 174xCEM cells are a fusion product of human B-cell line 721.174 and a human T-cell line CEM. 293T is an epithelial cell line derived from human embryonic kidney cells and expressing large T antigen. Information about cell lines is taken from https://aidsreagent.org/ and http://www.lgcstandards-atcc.org/.

293T (DSMZ-German Collection of Microorganisms and Cell Cultures, ACC 635) cells were maintained in Dulbecco's modified Eagle medium (DMEM, Pan Biotech) supplemented with 10% fetal calf serum (Biochrom, FCS) and 1% of 100× concentrated penicillin/streptomycin (pen/strep) mix (Pan Biotech). For subculturing, cells were detached by resuspension in phosphate-buffered saline (PBS [293T]) or incubation with trypsin/EDTA solution (Pan Biotech). The human T-cell lines 174xCEM (NIH AIDS Reagent Program, NIH272, (49)), PM1 (50), Sup-T1 (NIH AIDS Reagent Program, NIH100, (51)) and Jurkat (NIH AIDS Reagent Program, NIH177, (52)) were maintained in Roswell Park Memorial Institute 1640 medium (RPMI, Pan Biotech) supplemented with 10% FCS and 1% of 100× concentrated pen/strep mix. For subculturing, culture medium containing the suspension cells was centrifuged (600 × *g*, 10 min, room temperature). Then, the supernatant was discarded and pelleted cells were resuspended in 10 ml RPMI medium. Further, 1 ml of this suspension was added to a new culture flask and filled up with 19 ml of RPMI medium.

Cellular tRNA levels for $tRNA_{UAA}^{Leu}$, $tRNA_{CAG}^{Leu}$, $tRNA_{UAC}^{Val}$ and $tRNA_{CAC}^{Val}$ were quantified using a strategy published by (53). Total cellular RNA was extracted using the RNeasy Mini Kit (Qiagen) according to the manufacturer's protocol. After elution, the RNA content was determined spectrophotometrically. To eliminate potentially co-isolated DNA from the samples, 0.5 μg RNA was incubated with DNase I (New England Biolabs) in a final volume of 10 μl for 30 min at 37°C and finally heated to 65°C for 5 min to inactivate the enzyme. The primer for the reverse transcription entailed a tRNA-specific sequence and a stem-loop sequence (53). The tRNA-specific primer was the same for $tRNA_{UAA}^{Leu}$ and $tRNA_{CAG}^{Leu}$ (complementary to positions 47–55) and different for $tRNA_{CAC}^{Val}$ and $tRNA_{UAC}^{Val}$ (complementary to positions 62–70) (Supplementary Table S5). cDNA synthesis was performed as described in the manufacturer's instructions (for gene-specific primers) using the SuperScript III First-Strand Synthesis System (ThermoFisher Scientific) and 5 μl of DNase I-digested RNA (0.25 μg). Input RNA was removed by incubation with RNase H. To determine the levels of the tRNAs, $tRNA_{UAA}^{Leu}$, $tRNA_{CAG}^{Leu}$, $tRNA_{UAC}^{Val}$ and $tRNA_{CAC}^{Val}$ as well as 18S rRNA (housekeeping gene control), quantitative PCR (qPCR) was performed employing the QuantiTect SYBR Green Kit (Qiagen) according to the manufacturer's protocol on a Rotorgene Q device (Qiagen). The primers used for qPCR were taken from (53); the forward primer for the qPCR is highly specific to each tRNA and the reverse primer is universal (Supplementary Table S5). For each run, technical triplicates were analyzed for each sample and reactions containing water instead of template cDNA were used as negative control. Cycle conditions were chosen as follows: one cycle at 95°C for 15 min, followed by 45 cycles consisting of 15 s at 94°C, 30 s at 60°C and 30 s at 72°C. Finally, a linear temperature increase from 60 to 90°C with a ramp of 1°C per step and each step lasting 5 s was performed to obtain a melting curve for each reaction. In order to compare $tRNA_{UAA}^{Leu}$/$tRNA_{CAG}^{Leu}$ and RNA_{UAC}^{Val}/ $tRNA_{CAC}^{Val}$ tRNA ratio between cell lines, cycle threshold (c_t) values for each tRNA were normalized against the respective c_t values for 18S rRNA.

RESULTS

Two regimes for –1FS on the gag-pol slippery site

We first aimed to solve the mechanism of –1FS on the HIV-1 mRNA. For the mechanistic work, we used the fully reconstituted translation system from *E. coli*, because the overall efficiency and the ratio of the FLR and FFR products is similar in mammalian cells and in *E. coli* (5,15,23,24), the functional centers of the ribosomes where frameshifting takes place are highly conserved between eukaryotes and prokaryotes (54), and it is not feasible to prepare materials for the reconstituted eukaryotic translation system in amounts needed for this type of analysis. We first tested the potential routes for frameshifting. The model HIV-1 gag-pol mRNA encompasses the natural frameshifting site with the translation start codon AUG three codons upstream of the slippery site (Figure 1B). We formed a 70S initiation complex with the mRNA and $fMet\text{-}tRNA^{fMet}$ and started translation by the addition of ternary complexes of elongation factor (EF)-Tu–GTP with the desired combination of purified aa-tRNAs and EF-G–GTP. Consecutive amino acid incorporation results in a 0-frame peptide fMet-Gln-Ala-Asn-Phe-Leu-Gly (MQANFLG) and the –1-frame peptides fMet-Gln-Ala-Asn-Phe-Leu-Arg (MQANFLR) or fMet-Gln-Ala-Asn-Phe-Phe-Arg (MQANFFR). Peptides were analyzed by reversed-phase HPLC (RP-HPLC) (Supplementary Figure S1). The overall frameshifting efficiency was determined as a yield of –1-frame Arg incorporation relative to the sum of –1- and 0-frame peptides. With the mRNA containing a native slippery sequence, a large fraction of peptides contains Arg (Figure 1B), indicating efficient –1FS. As expected, the U_4C mutation, which changes the SS1 sequence to U UUC UUA (5), abolishes FS (Figure 1B and Supplementary Figure S3A).

In principle, –1FS can occur at the decoding step of the translation elongation cycle, when only peptidyl-tRNA is bound in the P site of the ribosome while the A site is vacant (15,55), or during translocation, when two tRNAs together with the mRNA move through the ribosome (56–59). If slippage occurred during decoding, the –1FS efficiency must depend on the competition between the 0-frame and –1-frame aa-tRNAs, Leu-tRNA and Phe-tRNA, for binding at the UUUA sequence in SS1. In fact, the addition of $Leu\text{-}tRNA_{NAA}^{Leu}$ (*E. coli* tRNA that reads the UUA and UUG codons; the anticodon is indicated as a subscript; N is a post-transcriptionally modified nucleotide) dramatically lowers the –1FS efficiency from about 50% in the absence to 12% in the presence of $Leu\text{-}tRNA_{NAA}^{Leu}$ (Figure 1C). In contrast, a mixture of near-cognate Leu-tRNA isoacceptors that collectively read the CUN family of Leu codons has no effect. The high –1FS efficiency observed in the absence of $Leu\text{-}tRNA_{NAA}^{Leu}$ indicates that ribosomes can slip into the –1-frame prior to, and independent of, Leu incorporation. By estimating the ratio of Leu, Phe and Arg incorporation into the –1-frame product, we can determine how the –1FS pathway changes with the $Leu\text{-}tRNA_{NAA}^{Leu}$ concentration (Figure 1D). In the absence of $Leu\text{-}tRNA_{NAA}^{Leu}$, only the FFR product is formed. Upon addition of $Leu\text{-}tRNA_{NAA}^{Leu}$, the FLR product becomes prevalent. Thus, frameshifting at the gag-pol slippery site can switch between two regimes and their prevalence depends on the concentration of the critical tRNA.

After Leu incorporation, the –1FS can follow different routes: it can take place either during $tRNA^{Leu}$ translocation or upon decoding of the following Gly codon. Again, if frameshifting took place during decoding, the 0-frame $Gly\text{-}tRNA^{Gly}$ and –1-frame $Arg\text{-}tRNA^{Arg}$ should compete for binding to the ribosome. This is, however, not observed, as the –1FS efficiency is independent of $Gly\text{-}tRNA^{Gly}$ and $Arg\text{-}tRNA^{Arg}$ concentrations (Figure 1E). This finding suggests that slippage and commitment to the new reading frame occur after Leu incorporation, but prior to decoding of the next codon by Gly- or Arg-tRNA. This is similar to the well-studied cases of –1FS on IBV 1a/1b and dnaX mRNAs, where slippage occurs at a late stage of translocation of the slippery-site tRNAs, and suggests a similar two-tRNA frameshifting mechanism (55–60).

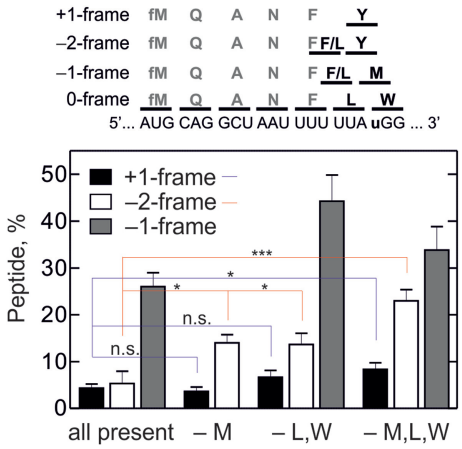

Figure 2. tRNA limitation results in –1, +1 and –2FS. Top panel shows the model mRNA and peptides synthesized in all frames. tRNAs for QANF were added to all translation reactions; in addition, Met (M), Leu (L), Trp (W) and Tyr (Y) were added in the 'all present' sample; –M, –L,W and –M,L,W indicate the aa-tRNAs that were omitted from the respective translation reaction. Positions of peaks were determined using [^{14}C]-labeled Tyr, Met, Leu or Trp. Two-tailed two-sample equal variance *t*-test was performed between marked samples; blue lines for +1 peptides and red lines for –2 peptides. n.s., not significant, * indicates $P \leq 0.05$, *** is $P \leq 0.001$.

The UUA codon is particularly rare in human cells and the respective Leu-tRNA$_{NAA}^{Leu}$ is underrepresented is some cell types (see below and (53)). Because formation of the –1-frame FFR product depends on the slippage at the 'hungry' UUA codon, we further tested whether this allows also –2 and +1FS. We note that normally such slippage events would lead to premature termination due to stop codons appearing in the –2 or +1 frames downstream of the frameshifting site and that such peptides are difficult to detect *in vivo*, but alternative slippage events could change the ratio between the Gag and Gag-Pol polyproteins. To distinguish between the products of the 0-, –1-, –2- and +1-FS, we changed the GGG (Gly) codon following the slippery site into UGG (Trp) (Figure 2 and Supplementary Figure S2), a mutation that does not affect the –1FS efficiency *in vivo* in human cells (10). In addition to the aa-tRNAs needed for translation of the MQANFL sequence, we added purified Trp-tRNA^{Trp} (W), elongator Met-tRNA^{Met} (M) and Tyr-tRNA^{Tyr} (Y). The expected 0-frame peptide is now MQANFLW and the –1-frame peptides are MQANFFM and MQANFLM. Shifting into the +1-frame should yield MQANFY and into the –2-frame MQANFFY and MQANFLY. When all required aa-tRNAs are present, the –1-frame peptides account for about 25% of product, consistent with the –1FS efficiency on the native gag-pol sequence in the presence of equimolar amounts of Leu-tRNA$_{NAA}^{Leu}$ and ribosomes (Figure 2), whereas the amounts of the +1 and –2 peptides are small. When Met-tRNA^{Met} is omitted, –2FS increases more than 2-fold, whereas the +1FS is not changed. –2FS is enhanced because –1FS exposes a 'hungry' Met codon in the A site, which favors the slippage. In the absence of Leu- and Trp-tRNA, –1FS efficiency increases to 45%, as expected; –2FS is unchanged; and again a small amount of the +1-frame product is formed. Without addition of Leu-, Trp- and Met-tRNA, the products of all three alternative frames are found. These data suggest that –2 and +1FS can occur when one or more of the aa-tRNAs are lacking; however, when all aa-tRNAs are available the –1FS pathway is prevalent.

Kinetics of FFR and FLR –1FS pathways

To understand the kinetic switch between the two different –1FS regimes, we monitored translation and –1FS efficiency using the codon-walk approach (56) in the absence and presence of Leu-tRNA$_{NAA}^{Leu}$. Rate constants were calculated by global fitting of the time courses using numerical integration according to the models shown in Figure 3. As additional information, we estimated the rate constants of Arg and Gly incorporation in independent experiments using model mRNAs without frameshifting elements (Supplementary Figure S3B and C).

For the –1FS model in the absence of Leu-tRNA$_{NAA}^{Leu}$, we introduced the steps that result in the formation of MQANF and the –1FS products MQANFF and MQANFFR. In addition, we introduced two reaction branches that account for the incomplete conversion of the 70S IC into products as follows. Because a fraction of initiation complexes does not enter translation, we introduced a step that accounts for this unproductive population (M $\rightarrow$ M$_n$, non-reactive). We also noticed that MQANF-tRNA^{Phe} in the absence of the A-site ligand tends to slowly dissociate from the ribosome (Supplementary Figure S3D); to account for this loss of peptidyl-tRNA we introduced the respective drop-off reaction. Global fitting of the time courses using numerical integration yielded a unique solution for all rate constants (Figure 3A and B; Supplementary Table S1). The step leading to the incorporation of the second Phe is slow, $\sim$0.01 s^{-1}, compared to all translation steps, which are at least 10 times faster. MQANFF peptides do not accumulate and are converted to the –1-frame peptide, MQANFFR. Thus, the incorporation of the second Phe residue is the rate-limiting step of frameshifting that commits the ribosome to –1-frame translation.

In the presence of Leu-tRNA$_{NAA}^{Leu}$, the ribosome synthesizes the 0-frame MQANF peptide and then either continues translation with Leu incorporation in the 0-frame or shifts into the –1-frame before Leu-tRNA$_{NAA}^{Leu}$ can bind. If Leu is incorporated, the 0-frame MQANFL product can partition between the 0-frame MQANFLG and the –1-frame MQANFLR. Global fitting of the time courses gives well-defined rate constants for most of the steps (Figure 3C–E). The rate-limiting step for the –1-frame FFR pathway has a rate constant of $\sim$0.03 s^{-1}, similar to that for the isolated FFR pathway. The efficiency of the FFR pathway depends on the ratio of the rates of –1-slippage and Leu-tRNA$_{NAA}^{Leu}$ binding. While the rate of slippage is constant, the rate of Leu-tRNA$_{NAA}^{Leu}$ binding increases with concentration. This explains why the addition of excess Leu-tRNA$_{NAA}^{Leu}$ inhibits the FFR route. At high concentrations of Leu-tRNA$_{NAA}^{Leu}$, the probability to bind Leu-tRNA$_{NAA}^{Leu}$ to the A site is higher than to slip into the –1 -frame. At this condition, the FFR pathway is suppressed and only the FLR pathway remains operational. After Leu incorporation, the –1FS efficiency of the FLR route is de-

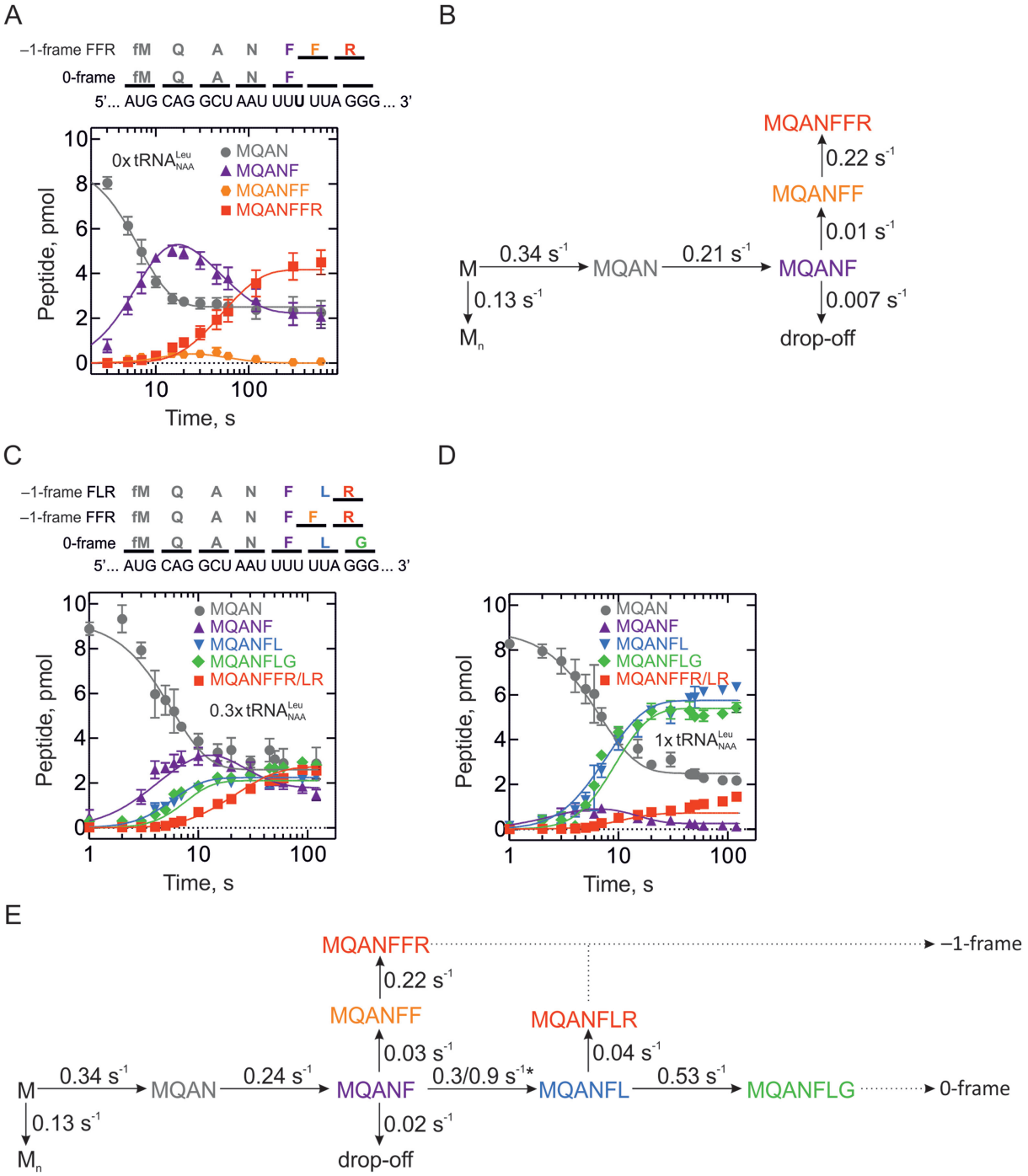

Figure 3. Kinetic mechanism of –1FS. (**A**) Time courses of translation in the absence of $tRNA_{NAA}^{Leu}$ reading the UUA codon. Peptides are MQAN (gray circles), MQANF (purple triangles), MQANFF (orange circles) and MQANFFR (red squares). Global fits are shown as continuous lines. The top panel shows amino acids in 0-frame and FFR –1-frame and respective codons on the mRNA. (**B**) Kinetic model of the FFR pathway in the absence of $tRNA_{NAA}^{Leu}$. Rates of all steps are calculated by global fitting. (**C** and **D**) Time courses of translation in the presence of limiting concentrations of $tRNA_{NAA}^{Leu}$ (C, 0.3-fold per ribosome) and near-saturating concentrations of $tRNA_{NAA}^{Leu}$ (D, 1-fold per ribosome). Peptides are MQAN (gray circles), MQANF (purple triangles), MQANFL (blue downward triangles), MQANFLG (green diamonds) and MQANFFR/MQANFLR (red squares). Global fits are shown as continuous lines. The top panel shows amino acids in 0-frame and –1-frame and respective codons on the mRNA. (**E**) Kinetic model of the FFR/FFL pathways in the presence of $tRNA_{NAA}^{Leu}$. Rates of all steps are calculated by global fitting. 0- and –1-frames are indicated by dotted arrows. *Incorporation of Leu-$tRNA_{NAA}^{Leu}$ is a bimolecular reaction and its rate depends on the concentration of $tRNA_{NAA}^{Leu}$. The two rates correspond to 0.3- and 1.0-fold excess of $tRNA_{NAA}^{Leu}$ over ribosomes, respectively.

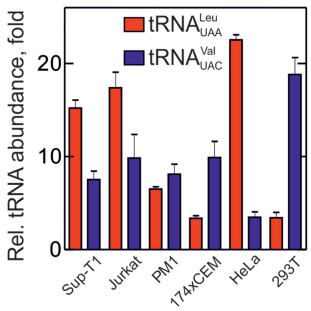

Figure 4. Relative abundance of tRNA isoacceptors in different cell types. Plotted is the ratio of $tRNA_{CAG}^{Leu}$ to $tRNA_{UAA}^{Leu}$ (red bars) and $tRNA_{CAC}^{Val}$ to $tRNA_{UAC}^{Val}$ (blue bars), which read frequent and rare codons, respectively, in human cell lines. Error bars represent S.E.M of three biological replicates with three technical replicates each. Experimental design of qRT-PCR was according to (53). Human cell lines are indicated below the graph. Sup-T1, Jurkat and PM1 are derived from human T-lymphocytes; 174xCEM is B-T-lymphocyte fusion; HeLa are derived from cervical epithelial carcinoma; 293T is a kidney epithelial cell line.

fined at the translocation step, because the partitioning between 0- and –1-frames takes place before decoding by Gly- and Arg-tRNAs (Figure 1E). The ratio of the rate constants of Gly and Arg incorporation (0.53 and 0.04 s^{-1}, respectively; Supplementary Table S1) gives the –1FS efficiency after Leu incorporation.

–1FS with native human aa-tRNA

Our finding that the Leu-$tRNA^{Leu}$ isoacceptor that reads the UUA codon affects the mechanism and efficiency of –1FS has prompted us to validate the key results in the eukaryotic system. First, we analyzed the relative abundance of human Leu-$tRNA^{Leu}$ that reads the UUA codon ($tRNA_{UAA}^{Leu}$) in total tRNA from different human cell types using qRT-PCR (Figure 4). HIV-1 mainly infects $CD4^+$ T-lymphocytes and macrophages (61). We determined the ratio of Leu-$tRNA_{UAA}^{Leu}$ to Leu-$tRNA_{CAG}^{Leu}$ reading the most abundant Leu codon CUG. Leu-$tRNA_{UAA}^{Leu}$ is 7–17-fold less abundant than Leu-$tRNA_{CAG}^{Leu}$ in cell lines derived from T lymphocytes, and about 20-fold in HeLa cells, whereas in other types of human cells the ratio is about 1:3 (Figure 4). The Leu-$tRNA_{UAA}^{Leu}$ concentration varies by as much as 10-fold, whereas for Leu-$tRNA_{CAG}^{Leu}$ the differences are smaller, except for HeLa cells, where the Leu-$tRNA_{CAG}^{Leu}$ concentration is increased (Supplementary Figure S4A). As a control, we quantified the relative abundance of Val-$tRNA^{Val}$ isoacceptors reading a rare GUA codon and an abundant GUG codon. The $tRNA_{UAC}^{Val}$ isoacceptor reading the rare codon is about 7–8 times less abundant than common $tRNA_{CAC}^{Val}$, except for the 293T epithelial cells, where the amount of $tRNA_{UAC}^{Val}$ is even lower (Figure 4). Because the relative abundance of $tRNA_{UAA}^{Leu}$ in HeLa cells is similar to that in cells used as a model for the HIV infection, we used total human tRNA purified from HeLa cells for the *in vitro* translation experiments described below.

We first tested how the HeLa aa-tRNA performs in translation when combined with EF-Tu and ribosomes from *E. coli* (Supplementary Figure S4B,C). The conformity of the human aa-tRNA to the codon usage of mammalian mRNA was validated by translation of an mRNA coding for bovine γB-crystallin. The codon usage of γB-crystallin matches the tRNA abundance of its eukaryotic host, but not of *E. coli* (62). With native human aa-tRNA, γB-crystallin mRNA is translated efficiently (Supplementary Figure S4D). Introducing synonymous mutations in the mRNA to match the codon usage in *E. coli* (62) reduces the yield of full-length product (Supplementary Figure S4D). The average translation rate of the gag-pol or the native γB-crystallin mRNA in our system is 0.5–0.7 aa/s (Supplementary Figure S4C).

We then translated a gag-pol mRNA fragment encompassing the region from the nearest native (elongator) AUG codon of the gag mRNA upstream of the SS1, the SS1 with its downstream SL1 and the second putative FS site, pSS2, with a 32-nt downstream sequence, which is predicted to form a SL (pSL2) (Figure 5A). To distinguish 0- and –1-frame translation products, we introduced a stop codon UAG in the 0-frame to obtain a peptide 52 amino acids (aa) in length; –1FS results in a 120-aa peptide product. To identify potential –2FS products, we mutated all native stop codons in the –2-frame downstream of the pSS2 (mRNA denoted as no-stop). Translation of the no-stop mRNA leaves the product lengths in the 0- and –1-frames unchanged, but additionally yields a 120-aa –2-frame product. Despite their identical length, the –1-frame and –2-frame products have different electrophoretic mobility due to their different amino acid composition (Figure 5B and Supplementary Figure S4E).

The –1FS efficiency of the native gag-pol frameshifting sequence is 6–7% (Figure 5C–E), consistent with earlier *in-vivo* reports (10–13). Formation of 0-frame and –1-frame products starts after a 30-s delay that may be caused by an early translational pausing event (appearing as a prominent peptide band between 7 and 30 s of translation (Figure 5B and C; Supplementary Figure S4E). In contrast, the –2-frame product appears after a much longer delay of 120 s. At this time, the synthesis of the 0-frame product is already completed on most ribosomes, suggesting that the –2FS may arise on a fraction of ribosomes that undergo long translation pausing. Addition of exogenous Leu-$tRNA_{NAA}^{Leu}$ decreases the –1FS efficiency to 4% (Figure 5D and Supplementary Figure S4F). A similarly reduced FS efficiency is observed when the UUA codon is mutated to UUC, which does not interrupt the slippery run of six Us, but changes the identity of the tRNA reading the second slippery codon to the abundant $tRNA^{Phe}$ (Figure 5E). Thus, reassigning the second codon of the slippery site to an abundant tRNA has the same effect as adding excess of $tRNA_{NAA}^{Leu}$ to the native sequence. Shortening the slippery site to four U residues decreased FS to 2%. Disrupting SS1 alone or together with pSS2 diminishes the FS efficiency to about 1%, which is the background level of these experiments (Figure 5E and Supplementary Figure S5B).

Finally, we tested whether addition of Leu-$tRNA_{UAA}^{Leu}$ alters the frameshifting efficiency in a homologous reconstituted mammalian translation system. Ribosomal subunits (40S and 60S), initiation factors (eIF1A, eIF1, eIF2, eIF3, eIF4A, eIF4B, eIF5, and eIF5B) and Met-$tRNA_i$ were used to form the 80S initiation complex on an mRNA with an un-

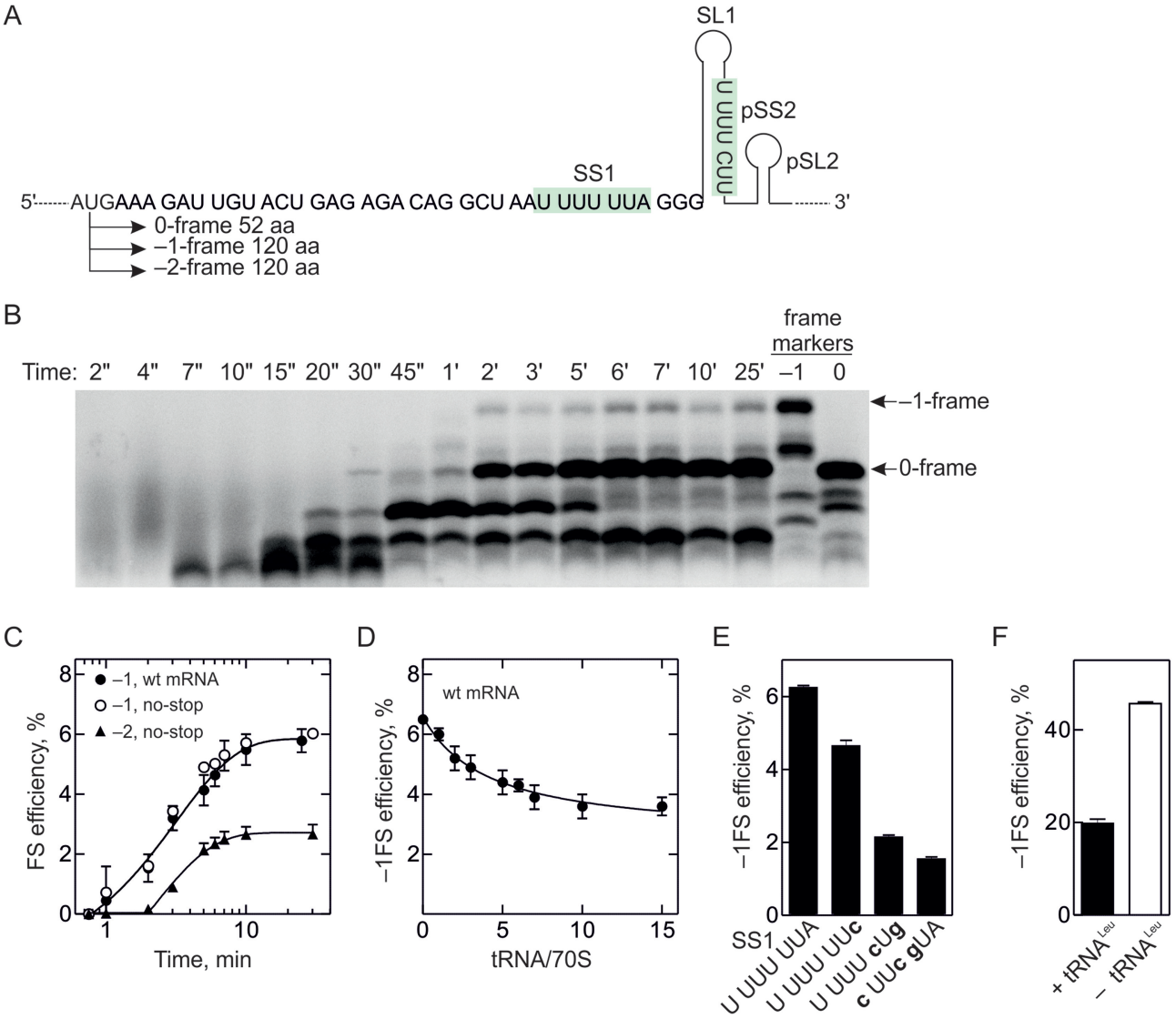

Figure 5. Translation and frameshifting with native human aa-tRNAs. (**A**) The mRNA used for translation experiments. SS1 and pSS2 are in highlighted light green, SL1 and the potential stem-loop element downstream of the pSS2 (pSL2) are shown. Sizes of 0-, –1- and –2-frame peptides formed upon translation of the mRNA are indicated. (**B**) Time course of 0-frame and –1-frame translation on wt mRNA. (**C**) Time courses of –1FS on wt mRNA (closed circles) as well as –1FS (open circles) and –2FS (closed triangles) on mRNA where all stop codons in –2-frame were mutated to sense codons (no-stop). (**D**) Concentration dependence of –1FS efficiency on exogenous $tRNA_{NAA}^{Leu}$ from *E. coli* measured on wt mRNA. (**E**) Effect of mutations in SS1 on –1FS. The background of the measurements is ±1%. The S.E.M was calculated from 3 to 5 independent experiments. (**F**) –1FS efficiency measured using a fully reconstituted homologous mammalian *in vitro* translation system with a gag-pol mRNA construct optimized for translation in eukaryotes. Translation was carried out in the presence (+ $tRNA^{Leu}$) and in the absence (– $tRNA^{Leu}$) of total Leu-$tRNA^{Leu}$ containing all isoacceptors in native ratios. The –1-frame peptide was identified based on [^{3}H]Arg incorporation.

structured 5'UTR coding for the SS1 and the SL1 fragment of HIV-1 (Figure 1A). To synthesize the 0-frame MVANFLG and the –1-frame MVANFLR peptides, we used the tRNA from HeLa cells aminoacylated with a mixture of the required amino acids with or without Leu; incorporation of the –1-frame Arg was monitored by the HPLC analysis (Supplementary Figure S4G). As controls, we included the mRNA coding for MVANFLR in 0-frame (–1-frame control), which provides the estimate for the maximum Arg incorporation, and the mRNA without the SS1 but with SL1 (0-frame control). The –1FS efficiency in this fully reconstituted eukaryotic translation system is about 20–25% in the presence of native amounts of $tRNA_{UAA}^{Leu}$ (Figure 5F and Supplementary Figure S4G). When leucine was omitted from the aminoacylation mixture, the –1FS efficiency increases to 40% (Figure 5F). Thus, Leu-$tRNA_{UAA}^{Leu}$ modulates –1FS efficiency on HIV mRNA also in the homologous mammalian translation system.

The putative second slippery sequence

To test the effect of mutations in the putative slippery sequence (pSS2), we introduced mutations that should make pSS2 either more or less slippery (Figure 6 and Supplementary Figure S5). As long as the SS1 sequence is un-

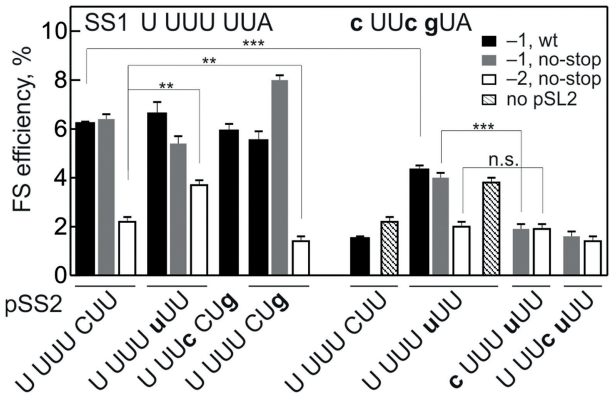

Figure 6. Interplay between SS1 and pSS2. SS1 sequences are shown above the bars, pSS2 sequences are indicated below the graph. –1FS is determined with wt mRNA (black bars) or with no-stop mRNA (gray bars); –2FS is measured with no-stop mRNA (white bars); the absence of pSL2 is indicated by textured pattern. Two-tailed two-sample equal variance *t*-test was performed between marked samples. n.s. means not significant, ** indicates $P \leq 0.01$, *** indicates $P \leq 0.001$.

changed, mutations in pSS2 have little effect on overall –1FS, but change the –2FS efficiency, which, in turn, leads to slight variations in –1FS. The –2FS efficiency is higher when both SS1 and pSS2 are slippery, suggesting that –2FS results from dual –1-slippage on both sites rather than from –2-slippage on pSS2 alone. Replacing the rare CUU codon in pSS2 with the abundant CUG reduces –2FS indicating that the second slippage is due to 'hungry' FS on pSS2. When the U-string in SS1 is disrupted, the frameshifting efficiency is higher in the construct where pSS2 is slippery compared to the native sequence. The presumed secondary structure of the mRNA downstream of pSS2 (Supplementary Figure S5) has no effect. Disruption of both slippery sites decreases frameshifting to background levels. Thus, pSS2 supports a low-level FS event that can rescue HIV-1 when SS1 is mutated, but also causes –2FS, which in the native sequence leads to premature termination of translation.

DISCUSSION

Kinetic mechanism of frameshifting on the gag-pol mRNA

We show that –1FS on HIV-1 mRNA operates in two regimes, one that is caused by a limitation of the UUA-specific Leu-tRNA isoacceptor and leads to the FFR –1-frame product, and another where ribosomes slip during $tRNA^{Phe}$–$tRNA^{Leu}$ translocation over the slippery site codons, yielding the FLR –1-frame product. The switch between the two regimes is modulated by the availability of the UUA-specific $tRNA^{Leu}$, which we show to be rare in cell lines derived from human immune cells. This notion is supported by *in vivo* experiments indicating that limitation of Leu in the culture media leads to increased –1FS in *E. coli* (15). The exact –1FS efficiency on the gag-pol mRNA differs depending on the type of model system, a phenomenon that has been noted before and attributed to different translation rates *in vivo* and *in vitro* (18,19,63,64); presumably, the presence of the bulk aa-tRNA also plays a role (compare Figures 1C and 5C). The UAA-specific Leu-tRNA modulates the –1FS efficiency in *E. coli*, mammalian or hybrid translation systems, which underscores the notion that this frameshifting mechanism is universally conserved.

The ribosome can also slip into the –1-, –2-, or +1-frames when some aa-tRNAs are lacking, but when all aa-tRNAs are supplied the –1-product is predominant. Similarly, translation of the *E. coli* dnaX mRNA can lead to slippages into the –2-, +2- or –4-frames when aa-tRNAs are in limiting supply (55,58). In the case of dnaX, the switch to 'hungry' frameshifting may be caused by unfavorable conditions, e.g. amino acid starvation (55,65–67). In contrast, HIV-1 can use both pathways constitutively due to the inherently low concentration of the key $tRNA_{UAA}^{Leu}$ isoacceptor in the relevant human cells. The fraction of –2PRF (25), which normally does not result in functional HIV products, may play a role in conjunction with the transcription slippage of the reverse transcriptase (68).

Role of the $tRNA_{UUA}^{Leu}$

As the ratio of the Gag and Gag-Pol products is crucial for virus propagation (6–9), HIV-1 must have evolved to achieve the desired –1FS efficiency at the concentrations of $tRNA_{UAA}^{Leu}$ prevalent in human cells. The UUA codon is rare in the human genome, as are all other A-ending codons. The respective cognate $tRNA_{UAA}^{Leu}$ is significantly underrepresented in the tRNA pool as compared to $tRNA_{CAG}^{Leu}$ that reads the abundant CUG codon (Figure 4) (53). While in eukaryotes the tRNA expression is tissue-specific, the relative expression of tRNA isoacceptors in some tissues shows statistically significant correlation to the codon usage of tissue-specific genes (69). The low relative abundance of $tRNA_{UAA}^{Leu}$ in the lymphocyte-derived cell types may be a result of adaptation to the codon usage in these cells. On the other hand, the rare UUA codon accounts for 45% of all Leu codons in late-expressing HIV-1 genes including *gag* and *pol* (70–72). Expression of the late HIV genes would increase the demand for a $tRNA_{UAA}^{Leu}$ that is rare in the respective cells, which may delay the decoding at any UUA codon, including the key codon in the slippery sequence. When the delivery to the UUA codon at the slippery site is too slow, the ribosome switches to the FFR route leading to robust –1FS. The codon usage disparity between HIV and its human host can be utilized to disrupt the late stage of virus production (73). For example, the interferon-induced antiviral protein Schlafen 11 (SLFN11) selectively abrogates the expression of late viral proteins in a codon-usage-dependent manner (73). SLFN11 induces specific cleavage of tRNAs with a long variable loop, which include all serine and leucine tRNAs. If the already rare tRNA, such as $tRNA_{UAA}^{Leu}$, is further reduced, tRNA availability might manifest as the rate-limiting step in the synthesis of proteins involving those tRNAs (73). A tRNA-dependent modulation of frameshifting was also reported within the expanded CAG stretch in the huntingtin gene (74): the translation of expanded CAG repeats in mutant huntingtin exon 1 leads to a depletion of charged Gln-$tRNA_{CUG}^{Gln}$ that pairs to the CAG codon, which results in translational frameshifting. The frameshifting frequency varies strongly among different cell lines and is higher in cells with intrinsically lower concentrations of $tRNA_{CUG}^{Gln}$ (74), which emphasizes the

biological significance of tRNA concentrations in modulating frameshifting efficiencies.

The second slippery site

Anti-HIV therapy with protease inhibitors leads to accumulation of mutations in the HIV-1 protease that impair the recognition of its specific cleavage sites. To allow for polyprotein maturation by the mutated protease, secondary mutations arise at the pSS2, which harbors the p1/p6 cleavage site of Gag polyprotein (75–79). The C_5U mutation in pSS2 substitutes Leu with Phe, which enhances van der Waals interactions between the substrate and the mutant protease, thereby increasing the protease activity by about 10-fold (80). The same mutation produces a slippery sequence that can support –1FS, but the role of pSS2 depends on the sequence of SS1. With native SS1, the joint activity of SS1 and pSS2 is not different from SS1 alone, but when SS1 is mutated to a non-shifty sequence, the C_5U mutation in the pSS2 is sufficient to support a level of –1FS that may be sufficient for virus propagation. The finding that pSS2 can alleviate the detrimental effects of SS1 mutations is consistent with previous *in vitro* and *in vivo* reports (26–30). Interestingly, during antiviral therapy, drug-resistant herpes simplex viruses also develop an unusual slippery site that supports both –1 and +1FS at levels sufficient for virus replication and pathogenicity despite the treatment (81,82). Similarly, the C_5U mutation in the pSS2 of gag-pol HIV-1 mRNA does not only modulate the FS efficiency, but also improves the activity of mutant proteases that emerge upon protease inhibitor treatment. The evolutionary pressure that has led to the conservation of pSS2 in HIV-1 is not known, but this sequence seems to allow rapid adaptation to anti-viral therapy (31). Thus, HIV-1 constitutively uses different FS regimes that have evolved to ensure a low but crucial level of FS required for its proliferation.

SUPPLEMENTARY DATA

Supplementary Data are available at NAR Online.

ACKNOWLEDGEMENTS

We thank Prof. Wolfgang Wintermeyer for critical reading of the manuscript, Prof. Tatyana Pestova for introducing us to eukaryotic translation and providing the expression constructs, Prajwal Karki for providing RF1, Dr. Dmitry Burakovskiy for providing eEF1A and eEF2, Dr. Neva Caliskan for participation in the initial phase of the project, and Anna Pfeifer, Olaf Geintzer, Sandra Kappler, Christina Kothe, Inga Nehlmeier, Theresia Niese, Tanja Wiles, Franziska Hummel, Tessa Hübner, Vanessa Herold and Michael Zimmermann for expert technical assistance. The following reagents were obtained through the National Institutes of Health AIDS Reagent Program, Division of AIDS, National Institute of Allergy and Infectious Diseases, National Institutes of Health: 174xCEM cells from Dr. Peter Cresswell, Sup-T1 cells from Dr. Dharam Ablashi, and Jurkat Clone E6–1 cells from Dr. Arthur Weiss. HeLa S10 cytoplasmic cell lysates were provided by the fermentation facility of Max Planck Institute for Biophysical Chemistry, Göttingen, Germany.

Author Contributions: N.K. prepared materials and performed most of experiments; A.G. performed experiments with the mammalian reconstituted translation system; M.H. performed qRT-PCR experiments; all authors conceived the research, designed experiments and analyzed the data; N.K. and M.V.R. wrote the paper with contributions of all authors.

FUNDING

Deutsche Forschungsgemeinschaft [SFB860, Leibniz Prize to M.V.R.]; Boehringer Ingelheim Fonds, PhD Fellowship [to N.K.]. Funding for open charge: MPG.
Conflict of interest statement. None declared.

REFERENCES

1. Plant,E.P. (2012) In: Garcia,PM (ed). *Viral Genomes - Molecular Structure, Diversity, Gene Expression Mechanisms and Host-Virus Interactions*. Intech.
2. Atkins,J.F., Loughran,G., Bhatt,P.R., Firth,A.E. and Baranov,P.V. (2016) Ribosomal frameshifting and transcriptional slippage: From genetic steganography and cryptography to adventitious use. *Nucleic Acids Res.*, **44**, 7007–7078.
3. Brierley,I., Gilbert,R. and Pennell,S. (2010) In: Atkins,JF and Gesteland,RF (eds). *Recoding: Expansion of decoding rules enriches gene expression*. Springer-Verlag, NY, pp. 149–174.
4. Advani,V.M. and Dinman,J.D. (2016) Reprogramming the genetic code: the emerging role of ribosomal frameshifting in regulating cellular gene expression. *Bioessays*, **38**, 21–26.
5. Jacks,T., Power,M.D., Masiarz,F.R., Luciw,P.A., Barr,P.J. and Varmus,H.E. (1988) Characterization of ribosomal frameshifting in HIV-1 gag-pol expression. *Nature*, **331**, 280–283.
6. Park,J. and Morrow,C.D. (1991) Overexpression of the gag-pol precursor from human immunodeficiency virus type 1 proviral genomes results in efficient proteolytic processing in the absence of virion production. *J. Virol.*, **65**, 5111–5117.
7. Karacostas,V., Wolffe,E.J., Nagashima,K., Gonda,M.A. and Moss,B. (1993) Overexpression of the HIV-1 gag-pol polyprotein results in intracellular activation of HIV-1 protease and inhibition of assembly and budding of virus-like particles. *Virology*, **193**, 661–671.
8. Shehu-Xhilaga,M., Crowe,S.M. and Mak,J. (2001) Maintenance of the Gag/Gag-Pol ratio is important for human immunodeficiency virus type 1 RNA dimerization and viral infectivity. *J. Virol.*, **75**, 1834–1841.
9. Biswas,P., Jiang,X., Pacchia,A., Dougherty,J. and Peltz,S. (2004) The human immunodeficiency virus type 1 ribosomal frameshifting site is an invariant sequence determinant and an important target for antiviral therapy. *J. Virol.*, **78**, 2082–2089.
10. Mathew,S.F., Crowe-McAuliffe,C., Graves,R., Cardno,T.S., McKinney,C., Poole,E.S. and Tate,W.P. (2015) The highly conserved codon following the slippery sequence supports -1 frameshift efficiency at the HIV-1 frameshift site. *PLoS One*, **10**, e0122176.
11. Plant,E.P. and Dinman,J.D. (2006) Comparative study of the effects of heptameric slippery site composition on -1 frameshifting among different eukaryotic systems. *RNA*, **12**, 666–673.
12. Grentzmann,G., Ingram,J., Kelly,P., Gesteland,R. and Atkins,J. (1998) A dual-luciferase reporter system for studying recoding signals. *RNA*, **4**, 479–565.
13. Cassan,M., Delaunay,N., Vaquero,C. and Rousset,J.P. (1994) Translational frameshifting at the gag-pol junction of human immunodeficiency virus type 1 is not increased in infected T-lymphoid cells. *J. Virol.*, **68**, 1501–1508.
14. Wilson,W., Braddock,M., Adams,S.E., Rathjen,P.D., Kingsman,S.M. and Kingsman,A.J. (1988) HIV expression strategies: ribosomal frameshifting is directed by a short sequence in both mammalian and yeast systems. *Cell*, **55**, 1159–1169.
15. Yelverton,E., Lindsley,D., Yamauchi,P. and Gallant,J.A. (1994) The function of a ribosomal frameshifting signal from human immunodeficiency virus-1 in Escherichia coli. *Mol. Microbiol.*, **11**, 303–313.

16. Brunelle,M., Payant,C., Lemay,G. and Brakier-Gingras,L. (1999) Expression of the human immunodeficiency virus frameshift signal in a bacterial cell-free system: influence of an interaction between the ribosome and a stem-loop structure downstream from the slippery site. *Nucleic Acids Res.*, **27**, 4783–4874.
17. Horsfield,J., Wilson,D., Mannering,S., Adamski,F. and Tate,W. (1995) Prokaryotic ribosomes recode the HIV-1 gag-pol-1 frameshift sequence by an E/P site post-translocation simultaneous slippage mechanism. *Nucleic Acids Res.*, **23**, 1487–1494.
18. Parkin,N.T., Chamorro,M. and Varmus,H.E. (1992) Human immunodeficiency virus type 1 gag-pol frameshifting is dependent on downstream mRNA secondary structure: demonstration by expression in vivo. *J. Virol.*, **66**, 5147–5151.
19. Reil,H., Kollmus,H., Weidle,U.H. and Hauser,H. (1993) A heptanucleotide sequence mediates ribosomal frameshifting in mammalian cells. *J. Virol.*, **67**, 5579–5584.
20. Dulude,D., Baril,M. and Brakier-Gingras,L. (2002) Characterization of the frameshift stimulatory signal controlling a programmed -1 ribosomal frameshift in the human immunodeficiency virus type 1. *Nucleic Acids Res.*, **30**, 5094–5102.
21. Bidou,L., Stahl,G., Grima,B., Liu,H., Cassan,M. and Rousset,J.P. (1997) In vivo HIV-1 frameshifting efficiency is directly related to the stability of the stem-loop stimulatory signal. *RNA*, **3**, 1153–1158.
22. Weiss,R.B., Dunn,D.M., Shuh,M., Atkins,J.F. and Gesteland,R.F. (1989) E. coli ribosomes re-phase on retroviral frameshift signals at rates ranging from 2 to 50 percent. *New Biol.*, **1**, 159–169.
23. Liao,P.Y., Choi,Y.S., Dinman,J.D. and Lee,K.H. (2011) The many paths to frameshifting: kinetic modelling and analysis of the effects of different elongation steps on programmed -1 ribosomal frameshifting. *Nucleic Acids Res.*, **39**, 300–312.
24. Cardno,T.S., Shimaki,Y., Sleebs,B.E., Lackovic,K., Parisot,J.P., Moss,R.M., Crowe-McAuliffe,C., Mathew,S.F., Edgar,C.D., Kleffmann,T. *et al.* (2015) HIV-1 and human PEG10 frameshift elements are functionally distinct and distinguished by novel small molecule modulators. *PLoS One*, **10**, e0139036.
25. Lin,Z., Gilbert,R.J. and Brierley,I. (2012) Spacer-length dependence of programmed -1 or -2 ribosomal frameshifting on a U6A heptamer supports a role for messenger RNA (mRNA) tension in frameshifting. *Nucleic Acids Res.*, **40**, 8674–8689.
26. Doyon,L., Payant,C., Brakier-Gingras,L. and Lamarre,D. (1998) Novel Gag-Pol frameshift site in human immunodeficiency virus type 1 variants resistant to protease inhibitors. *J. Virol.*, **72**, 6146–6150.
27. Girnary,R., King,L., Robinson,L., Elston,R. and Brierley,I. (2007) Structure-function analysis of the ribosomal frameshifting signal of two human immunodeficiency virus type 1 isolates with increased resistance to viral protease inhibitors. *J. Gen. Virol.*, **88**, 226–235.
28. Knops,E., Brakier-Gingras,L., Schulter,E., Pfister,H., Kaiser,R. and Verheyen,J. (2012) Mutational patterns in the frameshift-regulating site of HIV-1 selected by protease inhibitors. *Med. Microbiol. Immunol.*, **201**, 213–218.
29. Brierley,I. and Dos Ramos,F.J. (2006) Programmed ribosomal frameshifting in HIV-1 and the SARS-CoV. *Virus Res.*, **119**, 29–42.
30. Garcia-Miranda,P., Becker,J.T., Benner,B.E., Blume,A., Sherer,N.M. and Butcher,S.E. (2016) Stability of HIV frameshift site RNA correlates with frameshift efficiency and decreased virus infectivity. *J. Virol.*, **90**, 6906–6917.
31. Baril,M., Dulude,D., Gendron,K., Lemay,G. and Brakier-Gingras,L. (2003) Efficiency of a programmed -1 ribosomal frameshift in the different subtypes of the human immunodeficiency virus type 1 group M. *RNA*, **9**, 1246–1253.
32. Cunha,C.E., Belardinelli,R., Peske,F., Holtkamp,W., Wintermeyer,W. and Rodnina,M.V. (2013) Dual use of GTP hydrolysis by elongation factor G on the ribosome. *Translation*, **1**, e24315.
33. Doerfel,L.K., Wohlgemuth,I., Kothe,C., Peske,F., Urlaub,H. and Rodnina,M.V. (2013) EF-P is essential for rapid synthesis of proteins containing consecutive proline residues. *Science*, **339**, 85–88.
34. Donly,B.C., Edgar,C.D., Williams,J.M. and Tate,W.P. (1990) Tightly controlled expression systems for the production and purification of Escherichia coli release factor 1. *Biochem. Int.*, **20**, 437–443.
35. Florin,T., Maracci,C., Graf,M., Karki,P., Klepacki,D., Berninghausen,O., Beckmann,R., Vazquez-Laslop,N., Wilson,D.N., Rodnina,M.V. *et al.* (2017) An antimicrobial peptide that inhibits translation by trapping release factors on the ribosome. *Nat. Struct. Mol. Biol.*, **24**, 752–757.
36. Savelsbergh,A., Katunin,V.I., Mohr,D., Peske,F., Rodnina,M.V. and Wintermeyer,W. (2003) An elongation factor G-induced ribosome rearrangement precedes tRNA-mRNA translocation. *Mol. Cell*, **11**, 1517–1523.
37. Mittelstaet,J., Konevega,A.L. and Rodnina,M.V. (2013) A kinetic safety gate controlling the delivery of unnatural amino acids to the ribosome. *J. Am. Chem. Soc.*, **135**, 17031–17038.
38. Milon,P., Konevega,A.L., Peske,F., Fabbretti,A., Gualerzi,C.O. and Rodnina,M.V. (2007) Transient kinetics, fluorescence, and FRET in studies of initiation of translation in bacteria. *Methods Enzymol.*, **430**, 1–30.
39. Rodnina,M.V., Savelsbergh,A., Matassova,N.B., Katunin,V.I., Semenkov,Y.P. and Wintermeyer,W. (1999) Thiostrepton inhibits turnover but not GTP hydrolysis by elongation factor G on the ribosome. *Proc. Natl. Acad. Sci. U.S.A.*, **96**, 9586–9590.
40. Korencic,D., Soll,D. and Ambrogelly,A. (2002) A one-step method for in vitro production of tRNA transcripts. *Nucleic Acids Res.*, **30**, e105.
41. Kothe,U., Paleskava,A., Konevega,A.L. and Rodnina,M.V. (2006) Single-step purification of specific tRNAs by hydrophobic tagging. *Anal. Biochem.*, **356**, 148–150.
42. Mullis,K.B. (1990) Target amplification for DNA analysis by the polymerase chain reaction. *Ann. Biol. Clin.*, **48**, 579–582.
43. Tabor,S. and Richardson,C.C. (1985) A bacteriophage T7 RNA polymerase/promoter system for controlled exclusive expression of specific genes. *Proc. Natl. Acad. Sci. U.S.A.*, **82**, 1074–1078.
44. Milligan,J.F., Groebe,D.R., Witherell,G.W. and Uhlenbeck,O.C. (1987) Oligoribonucleotide synthesis using T7 RNA polymerase and synthetic DNA templates. *Nucleic Acids Res.*, **15**, 8783–8798.
45. Johnson,K.A. (2009) Fitting enzyme kinetic data with KinTek Global Kinetic Explorer. *Methods Enzymol.*, **467**, 601–626.
46. Schagger,H. and von Jagow,G. (1987) Tricine-sodium dodecyl sulfate-polyacrylamide gel electrophoresis for the separation of proteins in the range from 1 to 100 kDa. *Anal. Biochem.*, **166**, 368–379.
47. Pestova,T.V. and Hellen,C.U. (2003) Coupled folding during translation initiation. *Cell*, **115**, 650–652.
48. Pisarev,A.V., Unbehaun,A., Hellen,C.U. and Pestova,T.V. (2007) Assembly and analysis of eukaryotic translation initiation complexes. *Methods Enzymol.*, **430**, 147–177.
49. Salter,R.D., Howell,D.N. and Cresswell,P. (1985) Genes regulating HLA class I antigen expression in T-B lymphoblast hybrids. *Immunogenetics*, **21**, 235–246.
50. Lusso,P., Cocchi,F., Balotta,C., Markham,P.D., Louie,A., Farci,P., Pal,R., Gallo,R.C. and Reitz,M.S. Jr (1995) Growth of macrophage-tropic and primary human immunodeficiency virus type 1 (HIV-1) isolates in a unique CD4+ T-cell clone (PM1): failure to downregulate CD4 and to interfere with cell-line-tropic HIV-1. *J. Virol.*, **69**, 3712–3720.
51. Ablashi,D.V., Berneman,Z.N., Kramarsky,B., Whitman,J. Jr, Asano,Y. and Pearson,G.R. (1995) Human herpesvirus-7 (HHV-7): current status. *Clin. Diagn. Virol.*, **4**, 1–13.
52. Weiss,A., Wiskocil,R.L. and Stobo,J.D. (1984) The role of T3 surface molecules in the activation of human T cells: a two-stimulus requirement for IL 2 production reflects events occurring at a pre-translational level. *J. Immunol.*, **133**, 123–128.
53. Wan Makhtar,W.R., Browne,G., Karountzos,A., Stevens,C., Bottrill,A.R., Mistry,S., Smith,E., Bushel,M., Pringle,J.H. *et al.* (2017) Short stretches of rare codons regulate translation of the transcription factor ZEB2 in cancer cells. *Oncogene*, **36**, 6640–6648.
54. Melnikov,S., Ben-Shem,A., Garreau de Loubresse,N., Jenner,L., Yusupova,G. and Yusupov,M. (2012) One core, two shells: bacterial and eukaryotic ribosomes. *Nat. Struct. Mol. Biol.*, **19**, 560–567.
55. Caliskan,N., Wohlgemuth,I., Korniy,N., Pearson,M., Peske,F. and Rodnina,M.V. (2017) Conditional switch between frameshifting regimes upon translation of dnaX mRNA. *Mol. Cell*, **66**, 558–567.
56. Caliskan,N., Katunin,V.I., Belardinelli,R., Peske,F. and Rodnina,M.V. (2014) Programmed -1 frameshifting by kinetic partitioning during impeded translocation. *Cell*, **157**, 1619–1631.
57. Chen,J., Petrov,A., Johansson,M., Tsai,A., O'Leary,S.E. and Puglisi,J.D. (2014) Dynamic pathways of -1 translational frameshifting. *Nature*, **512**, 328–332.

58. Yan,S., Wen,J.D., Bustamante,C. and Tinoco,I. Jr (2015) Ribosome excursions during mRNA translocation mediate broad branching of frameshift pathways. *Cell*, **160**, 870–881.
59. Kim,H.K., Liu,F., Fei,J., Bustamante,C., Gonzalez,R.L. Jr and Tinoco,I. Jr. (2014) A frameshifting stimulatory stem loop destabilizes the hybrid state and impedes ribosomal translocation. *Proc. Natl. Acad. Sci. U.S.A.*, **111**, 5538–5543.
60. Chen,C., Zhang,H., Broitman,S.L., Reiche,M., Farrell,I., Cooperman,B.S. and Goldman,Y.E. (2013) Dynamics of translation by single ribosomes through mRNA secondary structures. *Nat. Struct. Mol. Biol.*, **20**, 582–588.
61. Freed,E.O. (2001) HIV-1 replication. *Somat. Cell Mol. Genet.*, **26**, 13–33.
62. Buhr,F., Jha,S., Thommen,M., Mittelstaet,J., Kutz,F., Schwalbe,H., Rodnina,M.V. and Komar,A.A. (2016) Synonymous codons direct cotranslational folding toward different protein conformations. *Mol. Cell*, **61**, 341–351.
63. Kollmus,H., Honigman,A., Panet,A. and Hauser,H. (1994) The sequences of and distance between two cis-acting signals determine the efficiency of ribosomal frameshifting in human immunodeficiency virus type 1 and human T-cell leukemia virus type II in vivo. *J. Virol.*, **68**, 6087–6091.
64. Dinman,J.D., Ruiz-Echevarria,M.J., Czaplinski,K. and Peltz,S.W. (1997) Peptidyl-transferase inhibitors have antiviral properties by altering programmed -1 ribosomal frameshifting efficiencies: development of model systems. *Proc. Natl. Acad. Sci. U.S.A.*, **94**, 6606–6611.
65. Gallant,J. and Lindsley,D. (1993) Ribosome frameshifting at hungry codons: sequence rules, directional specificity and possible relationship to mobile element behaviour. *Biochem. Soc. Trans.*, **21**, 817–821.
66. Gallant,J.A. and Lindsley,D. (1998) Ribosomes can slide over and beyond "hungry" codons, resuming protein chain elongation many nucleotides downstream. *Proc. Natl. Acad. Sci. U.S.A.*, **95**, 13771–13776.
67. Gallant,J.A. and Lindsley,D. (1992) Leftward ribosome frameshifting at a hungry codon. *J. Mol. Biol.*, **223**, 31–40.
68. Penno,C., Kumari,R., Baranov,P.V., van Sinderen,D. and Atkins,J.F. (2017) Specific reverse transcriptase slippage at the HIV ribosomal frameshift sequence: potential implications for modulation of GagPol synthesis. *Nucleic Acids Res.*, **45**, 10156–10167.
69. Dittmar,K.A., Goodenbour,J.M. and Pan,T. (2006) Tissue-specific differences in human transfer RNA expression. *PLoS Genet.*, **2**, e221.
70. van Weringh,A., Ragonnet-Cronin,M., Pranckeviciene,E., Pavon-Eternod,M., Kleiman,L. and Xia,X. (2011) HIV-1 modulates the tRNA pool to improve translation efficiency. *Mol. Biol. Evol.*, **28**, 1827–1834.
71. Sharp,P.M., Cowe,E., Higgins,D.G., Shields,D.C., Wolfe,K.H. and Wright,F. (1988) Codon usage patterns in Escherichia coli, Bacillus subtilis, Saccharomyces cerevisiae, Schizosaccharomyces pombe, Drosophila melanogaster and Homo sapiens; a review of the considerable within-species diversity. *Nucleic Acids Res.*, **16**, 8207–8211.
72. Berkhout,B., Grigoriev,A., Bakker,M. and Lukashov,V.V. (2002) Codon and amino acid usage in retroviral genomes is consistent with virus-specific nucleotide pressure. *AIDS Res. Hum. Retroviruses*, **18**, 133–141.
73. Li,M., Kao,E., Gao,X., Sandig,H., Limmer,K., Pavon-Eternod,M., Jones,T.E., Landry,S., Pan,T., Weitzman,M.D. *et al.* (2012) Codon-usage-based inhibition of HIV protein synthesis by human schlafen 11. *Nature*, **491**, 125–128.
74. Girstmair,H., Saffert,P., Rode,S., Czech,A., Holland,G., Bannert,N. and Ignatova,Z. (2013) Depletion of cognate charged transfer RNA causes translational frameshifting within the expanded CAG stretch in huntingtin. *Cell Rep.*, **3**, 148–159.
75. Bally,F., Martinez,R., Peters,S., Sudre,P. and Telenti,A. (2000) Polymorphism of HIV type 1 gag p7/p1 and p1/p6 cleavage sites: clinical significance and implications for resistance to protease inhibitors. *AIDS Res. Hum. Retroviruses*, **16**, 1209–1213.
76. Larrouy,L., Lambert-Niclot,S., Charpentier,C., Fourati,S., Visseaux,B., Soulie,C., Wirden,M., Katlama,C., Yeni,P., Brun-Vezinet,F. *et al.* (2011) Positive impact of HIV-1 gag cleavage site mutations on the virological response to darunavir boosted with ritonavir. *Antimicrob. Agents Chemother.*, **55**, 1754–1757.
77. de Oliveira,T., Engelbrecht,S., Janse van Rensburg,E., Gordon,M., Bishop,K., zur Megede,J., Barnett,S.W. and Cassol,S. (2003) Variability at human immunodeficiency virus type 1 subtype C protease cleavage sites: an indication of viral fitness? *J. Virol.*, **77**, 9422–9430.
78. Banke,S., Lillemark,M.R., Gerstoft,J., Obel,N. and Jorgensen,L.B. (2009) Positive selection pressure introduces secondary mutations at Gag cleavage sites in human immunodeficiency virus type 1 harboring major protease resistance mutations. *J. Virol.*, **83**, 8916–8924.
79. Pettit,S.C., Henderson,G.J., Schiffer,C.A. and Swanstrom,R. (2002) Replacement of the P1 amino acid of human immunodeficiency virus type 1 Gag processing sites can inhibit or enhance the rate of cleavage by the viral protease. *J. Virol.*, **76**, 10226–10233.
80. Ozen,A., Lin,K.H., Kurt Yilmaz,N. and Schiffer,C.A. (2014) Structural basis and distal effects of Gag substrate coevolution in drug resistance to HIV-1 protease. *Proc. Natl. Acad. Sci. U.S.A.*, **111**, 15993–15998.
81. Pan,D. and Coen,D.M. (2012) Net -1 frameshifting on a noncanonical sequence in a herpes simplex virus drug-resistant mutant is stimulated by nonstop mRNA. *Proc. Natl. Acad. Sci. U.S.A.*, **109**, 14852–14857.
82. Griffiths,A. (2011) Slipping and sliding: frameshift mutations in herpes simplex virus thymidine kinase and drug-resistance. *Drug Resist. Updat.*, **14**, 251–259.